Observation of the Transition to Chaos in the Level Statistics of Diamagnetic Helium

K. Karremans, W. Vassen, and W. Hogervorst

Department of Physics and Astronomy, Vrije Universiteit, De Boelelaan 1081, 1081 HV Amsterdam, The Netherlands

(Received 20 August 1998)

We have investigated level statistics in constant-scaled-energy spectra of the diamagnetic helium atom. In a transversely laser-cooled beam metastable triplet atoms are excited to Rydberg states in the presence of a magnetic field, resolving all resonances. In the regime of regular classical motion level distributions obeying Poisson statistics are observed. Small deviations are attributed to scattering at the nonhydrogenic He^+ core as inferred from closed-orbit theory. The nearest-neighbor spacings in spectra in the chaotic regime demonstrate a clear shift towards Wigner statistics. [S0031-9007(98)07780-1]

PACS numbers: 05.45.+b, 03.65.Sq, 32.60.+i

The connection between classical mechanics and quantum theory via the correspondence principle breaks down for classically chaotic systems, as the concept of exponentially diverging trajectories does not exist in quantum mechanics [1]. Model systems, whose classical dynamics may be chaotic, such as the stadium billiard, the kicked rotor, and atoms in strong magnetic fields, have been investigated in detail, primarily theoretically. The Rydberg atom in a strong magnetic field is particularly suited to confront calculations with experimental results. Energy level statistics is considered to be a tool to observe a "fingerprint of chaos" in experimental spectra [1–4]. In this Letter we present experiments on diamagnetic helium Rydberg atoms in the regular and chaotic regime performed with a resolution sufficient to observe all spectral details. We will discuss small effects of the He^+ core on the observed level statistics applying closed-orbit theory. This analysis provides physical insight into the different features observed into the experimental spectra.

The hydrogen atom in a strong magnetic field is a nonintegrable system due to the different symmetries of Coulomb (spherical) and magnetic (cylindrical) interaction. At strong fields only two constants of motion (energy and z component of angular momentum) exist for this system with 3 degrees of freedom, a prerequisite for classical chaos. In our experiment $M_L = 0$ states are excited and therefore the Zeeman term vanishes. The nonrelativistic Hamiltonian (in a.u.) for $M_L = 0$ is

$$H = \frac{p^2}{2} - \frac{1}{r} + \frac{1}{8}\gamma^2(x^2 + y^2). \qquad (1)$$

Here γ represents the magnetic field. The diamagnetic term in the Hamiltonian becomes dominant at high excitation energy. The introduction of scaled variables $\tilde{r} = \gamma^{2/3} r$ and $\tilde{p} = \gamma^{-1/3} p$ [3] shows that the classical behavior of the system depends only on a single parameter, the scaled energy $\varepsilon = E\gamma^{-2/3}$ (E is the energy with respect to the ionization limit). In the field-free case ($\varepsilon = -\infty$) all classical electron trajectories are stable. Around $\varepsilon = -0.50$ numerical calculations show a smooth increase of the number of chaotic trajectories, up to $\varepsilon = -0.127$ when finally the last stable orbit, i.e., the orbit perpendicular to the magnetic field, turns chaotic.

The connection between classical trajectories and quantum mechanical spectra is made by closed-orbit theory [5]. Closed-orbit theory states that each electron orbit starting at and returning to the core region generates an oscillation in the photoabsorption spectrum. The spectrum, at constant scaled energy, contains a smooth background and a sum of oscillatory terms of the form

$$f(\varepsilon, \gamma) = C_k^n(\varepsilon) \sin(2\pi n \tilde{S}_k \gamma^{-1/3} - \psi_k^n). \qquad (2)$$

C_k^n, the recurrence amplitude of a closed orbit, contains information on the stability of the orbit and the geometry of excitation; $\tilde{S}_k$ is the classical scaled action and ψ_k^n is the recurrence phase. A summation over all orbits k and their repeated traversals n up to a maximum scaled action $\tilde{S}_{\max}$ reconstructs the spectrum with a resolution of $1/(2\tilde{S}_{\max})$ on a $\gamma^{-1/3}$ scale, which is related to the usual energy scale via $E = \varepsilon\gamma^{2/3}$.

From scaled-energy spectra a recurrence spectrum can be constructed using a Fourier transformation. The positions of the sharp resonances, with a width inversely proportional to the length of the scan, determine the scaled actions with high accuracy. The importance of scaled-energy spectroscopy was demonstrated earlier in various experiments [6–8]. In the interpretation of the recurrence spectra every resonance is attributed to one or more closed classical orbits and their multiple traversals. In contrast to stable orbits, for chaotic orbits an exponential decrease in the amplitude of multiple returns is expected. However, the frequency range required to resolve all individual classical orbits to observe such an exponential decrease has to our knowledge never been obtained in experiments nor in calculations.

Other methods to interpret spectra are based on the statistical behavior of the eigenstates. Nearest-neighbor statistics (NNS) is a convenient way to determine the difference between chaotic and regular spectra [1]. In a regular spectrum, under the condition that many n manifolds overlap (n is the principal quantum number), the absence of level repulsions (in hydrogen) will lead to Poisson statistics for the level spacing distribution:

$$P(s)_{\text{Poisson}} = e^{-s}, \qquad (3)$$

where $s = 1$ corresponds to the mean level spacing.

Chaotic spectra show the same statistical properties as Gaussian orthogonal ensembles of random matrices. The Wigner distribution, found for linear repulsion between energy levels, is a good approximation for NNS of these ensembles:

$$P(s)_{\text{Wigner}} = \frac{\pi}{2} s e^{-\pi s^2/4}. \quad (4)$$

The differences between the two types of distributions are most pronounced for small level spacings. In the regular NNS the largest probability corresponds to small spacings, where the chaotic distribution tends to zero. In the intermediate regime the best single parameter fit is obtained for a heuristic Brody distribution:

$$P(s;q)_{\text{Brody}} = \alpha(q+1)s^q e^{-\alpha s^{q+1}}, \quad (5)$$

with

$$\alpha = \left[\Gamma\left(\frac{q+2}{q+1}\right)\right]^{(q+1)}. \quad (6)$$

The Brody parameter can be tuned to interpolate smoothly between the limiting cases of Poisson ($q = 0$) and Wigner ($q = 1$) statistics, and is roughly related to the fraction of classical phase space occupied by chaotic orbits [4].

First laser experiments were carried out on diamagnetic hydrogen [6,8]. However, the resolution in these pulsed laser experiments was not sufficient to reveal all individual energy levels and, consequently, level statistics of experimental hydrogen spectra could not be investigated thus far. More accurate experiments are feasible with CW laser excitation of nonhydrogenic Rydberg atoms. A quantum defect, however, leads to anticrossings in such spectra and to an absence of short distances, which then gives rise to a deviation from Poisson statistics in the regular regime. For large quantum defects [$\delta(\text{mod } 1) \sim 0.5$] even in the regular regime Wigner distributions were observed in experiments on Rb Rydberg states in a magnetic field [9] as well as in calculations [10]. Similar observations were made in Li Rydberg states in an electric field [11]. The origin of this so-called core-induced chaos is fundamentally different, as can be understood from a semiclassical approach, where the core is simulated by a model potential that reproduces the quantum defect. This short-range potential results in the scattering of the excited electron from one stable hydrogenic orbit into another giving rise to sum-orbit peaks in the recurrence spectra of nonhydrogenic atoms [12]. In between core scattering events the motion is restricted to hydrogenic tori. Although the appearance of ergodic motion in the long time behavior of nonhydrogenic trajectories (for all $\delta \neq 0$) may justify the term "core-induced chaos," this approach completely neglects the pure quantum mechanical nature of the scattering process. Quantum numerical calculations on the dependence of NNS on δ were performed by Jans *et al.* [10]. In the limit of small δ (< 0.1) these calculations show a transition from nearly Poisson to Wigner statistics when the scaled energy is increased from $\varepsilon = -0.5$ to $\varepsilon = -0.1$. From odd-parity Li Rydberg spectra ($\delta = 0.05$), recorded at constant magnetic field, Poisson statistics in the regular regime ($-0.7 < \varepsilon < -0.5$) was deduced [13]. In a recent theoretical paper [14], it was mentioned that the choice of a too large bin size in this analysis obscured the observation of deviations from a Poisson distribution.

The small quantum defect of ^3P Rydberg series ($\delta = 0.068$) provides a good opportunity to study the transition to chaotic NNS in odd-parity helium. In our experiment $M_L = 0$ Rydberg states are excited from the metastable $2\,^3S$ state in a crossed laser-atomic beam experiment using a frequency-doubled cw dye laser, generating 3 mW of 260 nm UV light (linewidth < 2 MHz). In previous experiments [7] the diverging atomic beam (1.5 mrad) resulted in a Doppler-limited linewidth of 25 MHz FWHM, preventing the observation of details in the spectra. To reduce the Doppler width and to improve signal strength we now use a two-dimensionally transversely laser-cooled beam of atoms. The properties of this bright beam are described elsewhere [15]. Now the small divergence of the UV laser beam (0.5 mrad) is the limiting factor. Our final result is a linewidth of 8 MHz FWHM. The best compromise between an intense atomic beam and minimum stray electric fields in the excitation region is obtained for an interaction volume of ~ 1 mm^3. Laser cooling enhances the signal by a factor of 10. The magnetic field (up to 0.3 T) is generated by an electromagnet and is directed parallel to the atomic beam to minimize motional Stark effects. To keep the scaled energy constant, the magnetic field is adjusted after every laser step of 3 MHz. The laser frequency is accurately determined by recording the fringes of a 150 MHz etalon (at $\lambda = 520$ nm), resulting in an absolute accuracy in ε of 0.0005. The magnetic field is scanned from 0.3 to 0.25 T, which for a given ε determines the range of n values.

In the first experiment we recorded a series of scaled energy spectra at $\varepsilon = -0.70$ covering the range of principal quantum number $n = 79$ to 90. Part of this spectrum is shown in the upper part of Fig. 1, while the lower part shows an earlier measurement at lower magnetic field with an uncooled beam. The spectra overlap within 10 MHz, showing the accuracy of ε to be better than 0.0001. Large-scale calculations using the R-matrix formalism for helium at constant scaled energy [12] were performed to compare with the experimental data. At $\varepsilon = -0.7$, we find 474 theoretical resonances in the experimental range; we observe 475 peaks. The smallest distance between peaks in the calculated spectra (40 MHz) is easily resolved experimentally. To determine ε more accurately, numerical simulations were performed varying ε in steps of 0.0001. The best agreement with experiment is found for calculations at $\varepsilon = -0.7002$. Almost every experimental peak can be assigned to a theoretical one. Only a few peaks were lost in the background, while some extra peaks, induced by a weak residual electric field, give rise to spacings at relatively short distances (20–60 MHz). The stray

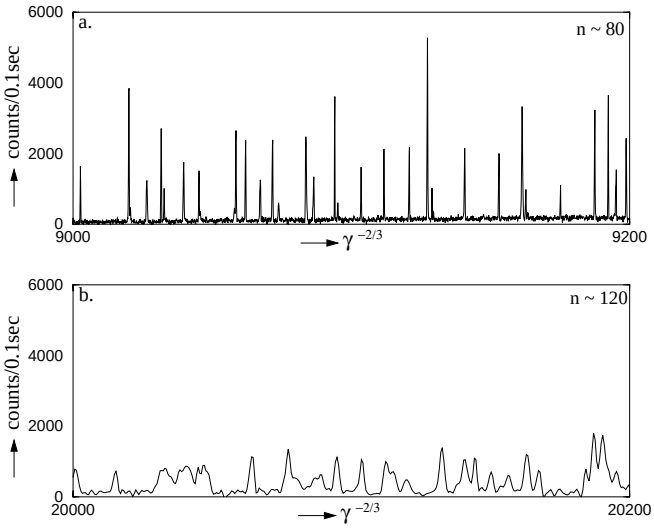

FIG. 1. The improved resolution of the present experimental setup. (a) Spectrum recorded with laser-cooled beam of He^* atoms. (b) Spectrum of uncooled beam. $\gamma^{-2/3}$ ranges with equal level distributions at $\varepsilon = -0.7$ are compared.

electric field is estimated to be smaller than 5 mV/cm from broadening of zero field resonances. In the presence of the magnetic field a few peaks showed a large sensitivity to a parallel electric field. After field compensation the parallel field component was reduced to less than 0.5 mV/cm. Conversion of the eigenenergies to a $\gamma^{-2/3}$ scale removes the variation in the density of states. The histograms of the separation between adjacent levels, normalized to mean level spacing, are presented in Fig. 2. Comparison with the Poisson-like hydrogen calculations (also shown) gives only in the first bin a significant difference. Our choice for a small bin size thus reveals the small deviation from Poisson statistics at $\varepsilon = -0.7$. This distribution fits to a Brody function with $q = 0.2$ ($q = 0$ for hydrogen), suggesting that the helium core induces some chaotic behavior. The recurrence spectrum at $\varepsilon = -0.7$ shown in Fig. 3 gives additional information about the origin of this slight deviation from Poisson statistics. In Fig. 3a this recurrence spectrum is mirror imaged with the result of hydrogen calculations, showing a striking resemblance. All peaks in the recurrence spectrum can be connected to classical closed orbits. A close examination of the experimental data, however, shows small additional peaks (Fig. 3b). Their position corresponds exactly with the sum of actions of two hydrogenic orbits (sum orbits). This is a clear manifestation of the process of core scattering. The low intensity of these peaks reflects the small probability of scattering on the nonhydrogenic helium core. This high resolution experiment demonstrates the difficulties to extract information on the stability of classical phase space from level statistics alone. Closed-orbit theory is required to reveal the dominant stable, classical orbits and to provide physical insight into the origin of the deviation from Poisson statistics produced by the quantum process of core scattering.

In a second experiment scaled energy spectra were recorded in the chaotic domain for $\varepsilon = -0.30$ in the same magnetic field range. The spectra become more dense due to the higher excitation energy, which also slightly affects the resolution. R-matrix calculations show, however, that only a single separation below the experimental resolution occurs. Few weak peaks could not be uncovered. Theoretically we expect 330 peaks in the energy range, while 335 were recorded experimentally. Again a weak parallel

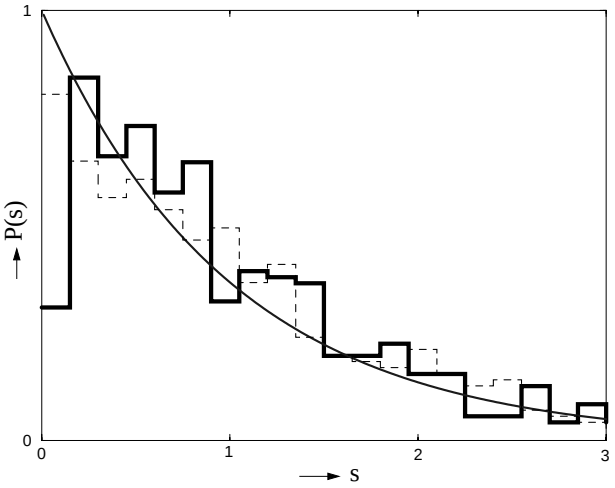

FIG. 2. Histograms of nearest-neighbor separations of experimental data (bold) and hydrogen calculations (dashed) at $\varepsilon = -0.7$. Poisson statistics (full curve) gives a good approximation of the hydrogen level distribution, whereas in the experiment anticrossings induce a deviation from Poisson statistics (in the first bin).

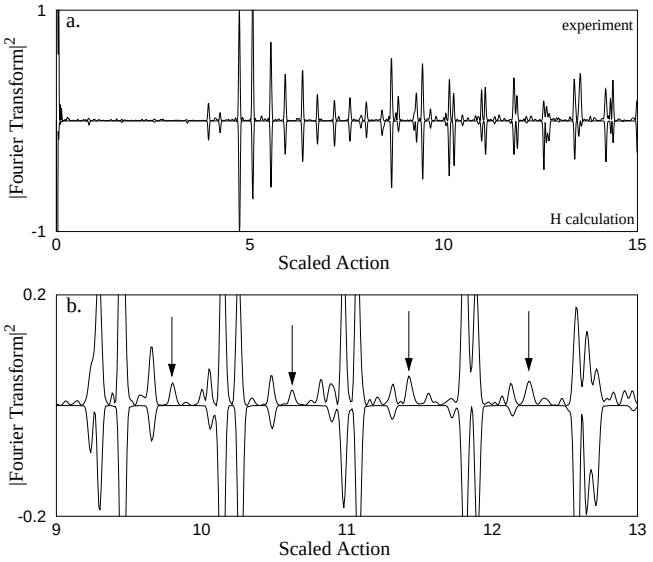

FIG. 3. (a) Comparison between experimental recurrence spectrum at $\varepsilon = -0.7$ with hydrogen calculations. All hydrogenic peaks can be attributed to classical orbits. (b) Magnification (5×) of part of the recurrence spectrum. In the experimental spectrum, extra peaks (arrows) appear exactly at the sum of actions of two hydrogenic orbits.

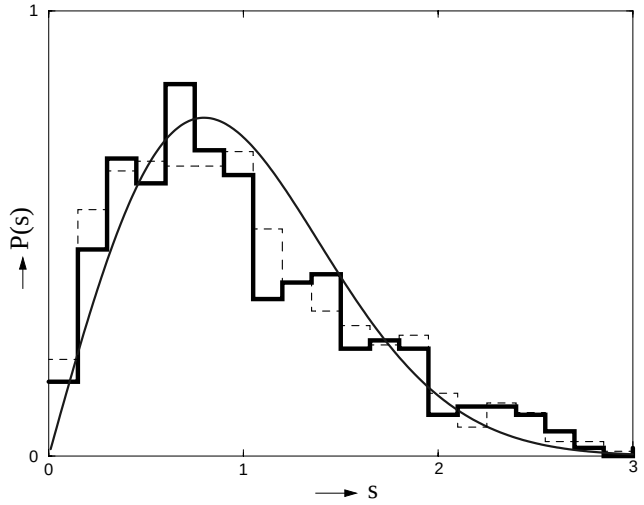

FIG. 4. Histograms of nearest-neighbor separations of experimental data (bold) and hydrogen calculations (dashed) at $\varepsilon = -0.3$. Wigner statistics (full curve) gives a good fit of the hydrogenic and experimental level distributions.

electric field induces extra peaks. The experimental NNS for $\varepsilon = -0.3$ is shown, together with the calculated distribution for hydrogen, in Fig. 4. The experimental curve is in good agreement with hydrogenic theory, also for small spacings. Fitting calculated distributions for hydrogen and helium to Brody functions at $\varepsilon = -0.3$ ($q = 0.8$ for both) shows no significant difference with the experimental distribution (also $q = 0.8$). Core-induced effects are now invisible in the NNS. The level repulsion induced by the magnetic field turns out to be much stronger than the anticrossings due to the quantum defect.

To summarize, we succeeded in extracting NNS from diamagnetic helium spectra at constant scaled energy in the classical regular ($\varepsilon = -0.7$) and the chaotic ($\varepsilon = -0.3$) regime. Because of the small quantum defect a nearly Poissonian distribution is found at $\varepsilon = -0.7$. The small deviation from the calculated hydrogenic level distribution is caused by a scattering process on the He^+ core. The observation of Wigner-like statistics at $\varepsilon = -0.3$ can be regarded as the experimental signature of chaos. To our knowledge, this is the first experimental observation of the transition to chaos in a quantum mechanical system.

We would like to thank J. Bouma for his excellent technical support and D. Delande for providing the computer code for the quantum calculation. Financial support from Foundation for Fundamental Research on Matter (FOM) is gratefully acknowledged.

[1] M. C. Gutzwiller, *Chaos in Classical and Quantum Mechanics* (Springer-Verlag, New York, 1990).
[2] D. Delande and J. C. Gay, Phys. Rev. Lett. **57**, 2006 (1986).
[3] H. Friedrich and D. Wintgen, Phys. Rep. **183**, 37 (1989).
[4] A. Hönig and D. Wintgen, Phys. Rev. A **39**, 5642 (1989).
[5] M. L. Du and J. B. Delos, Phys. Rev. A **38**, 1896 (1988).
[6] A. Holle, J. Main, G. Wiebusch, H. Rottke, and K. H. Welge, Phys. Rev. Lett. **61**, 161 (1988).
[7] T. van der Veldt, W. Vassen, and W. Hogervorst, Europhys. Lett. **21**, 9 (1993).
[8] J. Main, G. Wiebusch, K. Welge, J. Shaw, and J. B. Delos, Phys. Rev. A **49**, 847 (1994).
[9] H. Held, J. Schlichter, G. Raithel, and H. Walther, Europhys. Lett. **43**, 392 (1998).
[10] W. Jans, T. S. Monteiro, W. Schweizer, and P. A. Dando, J. Phys. A **26**, 3187 (1993).
[11] M. Courtney, H. Jiao, N. Spellmeyer, and D. Kleppner, Phys. Rev. Lett. **73**, 1340 (1994); M. Courtney, N. Spellmeyer, H. Jiao, and D. Kleppner, Phys. Rev. A **51**, 3604 (1995).
[12] D. Delande, K. T. Taylor, M. Halley, T. van der Veldt, W. Vassen, and W. Hogervorst, J. Phys. B **27**, 2771 (1994).
[13] G. R. Welch, M. M. Kash, C. Iu, L. Hsu, and D. Kleppner, Phys. Rev. Lett. **62**, 893 (1989).
[14] M. Courtney and D. Kleppner, Phys. Rev. A **53**, 178 (1996).
[15] W. Rooyakkers, W. Hogervorst, and W. Vassen, Opt. Commun. **123**, 321 (1996).